JOURNAL OF CELLULAR PHYSIOLOGY 201:470–482 (2004)

Chondrocyte Protein With a Poly-Proline Region (CHPPR) Is a Novel Mitochondrial Protein and Promotes Mitochondrial Fission

LAURA TONACHINI,[1] MASSIMILIANO MONTICONE,[1,2] CLAUDIA PURI,[3] CARLO TACCHETTI,[3] PAOLO PINTON,[4] ROSARIO RIZZUTO,[4] RANIERI CANCEDDA,[1,2] SARA TAVELLA,[2] AND PATRIZIO CASTAGNOLA[1]*

[1]*Istituto Nazionale per la Ricerca sul Cancro, Genova, Italy*
[2]*Dipartimento Oncologia, Biologia e Genetica, Università di Genova, Italy*
[3]*Dipartimento di Medicina Sperimentale, Sezione di Anatomia, e Centro di Oncologia Cellulare e Ultrastrutturale IFOM, Genoa, Italy*
[4]*Dip. di Medicina Sperimentale e Diagnostica, Sezione di Patologia Generale, Università di Ferrara, Italy*

We have recently identified a chondrocyte protein with a poly-proline region, referred to as CHPPR, and showed that this protein is expressed intracellularly in chick embryo chondrocytes. Conventional fluorescence and confocal localization of CHPPR shows that CHPPR is sorted to mitochondria. Furthermore, immunoelectron microscopy of CHPPR transfected cells demonstrates that this protein is mostly associated with the mitochondrial inner membranes. Careful analysis of CHPPR expressing cells reveals, instead of the regular mitochondrial tubular network, the presence of a number of small spheroid mitochondria. Here we show that the domain responsible for network–spheroid transition spans amino acid residues 182–309 including the poly-proline region. Functional analyses of mitochondrial activity rule out the possibility of mitochondrial damage in CHPPR transfected cells. Since cartilage expresses high levels of CHPPR mRNA when compared to other tissues and because CHPPR is associated with late stages of chondrocyte differentiation, we have investigated mitochondrial morphology in hypertrophic chondrocytes by MitoTracker Orange labeling. Confocal microscopy shows that these cells have spheroid mitochondria. Our data demonstrate that CHPPR is able to promote mitochondrial fission with a sequence specific mechanism suggesting that this event may be relevant to late stage of chondrocyte differentiation. J. Cell. Physiol. 201: 470–482, 2004.

We have recently characterized a cDNA encoding the protein chondrocyte protein with a poly-proline region (CHPPR) (Tonachini et al., 2002). This cDNA was isolated by a subtractive cDNA library screen of hypertrophic and proliferating chick chondrocytes. We showed that CHPPR mRNA is more abundant in chick embryo cartilage than in several other tissues and that in vitro and in vivo CHPPR gene expression increases with chondrocyte maturation (Tonachini et al., 2002). We also showed that in vitro parathyroid hormone peptide [PTH (1–34)] enhances the accumulation of CHPPR mRNA in this cell type (Tonachini et al., 2002). The CHPPR amino acid sequence contains a characteristic proline-rich region with a proline–proline–leucine–proline (PPLP, single letter amino acid code) motif (Tonachini et al., 2002). No other structural or functional motifs or domains so far characterized and available in public databases were identified in this protein. By BLAST analysis we determined that the cDNA insert of the isolated clone is the avian counterpart of a human partial cDNA, named KIAA0009 (Nomura et al., 1994). Since to our knowledge neither further characteristics nor expression data of KIAA0009 have been published, we consider KIAA0009 as the human CHPPR.

We demonstrated by both Western blot and immunohistochemistry analysis that CHPPR is localized intracellularly in chondrocytes (Tonachini et al., 2002). Here

Laura Tonachini and Massimiliano Monticone contributed equally to this work.

Contract grant sponsor: Consiglio Nazionale delle Ricerche, Rome (Italy) P.F. Biotecnologie; Contract grant number: 99.00524.PF49.

*Correspondence to: Patrizio Castagnola, Istituto Nazionale per la Ricerca sul Cancro, Largo R. Benzi 10, 16132 Genova, Italy. E-mail: patrizio.castagnola@istge.it

Received 27 June 2003; Accepted 11 February 2004

DOI: 10.1002/jcp.20126

we prove that CHPPR is a novel mitochondrial protein able to promote mitochondrial fission. In particular, we show that CHPPR transfected cells and cultured hypertrophic chondrocytes, expressing endogenous CHPPR, have spheroid mitochondria instead of a tubular mitochondrial network like other cell types. We have also demonstrated that a specific domain, including the proline rich region, is responsible for the mitochondrial fission activity of CHPPR. This effect is also observed in cells, transfected with constructs containing this domain, expressing low or comparable levels of mRNA with respect to cells transfected with fission incompetent CHPPR-derived constructs. We have also investigated whether the fission process induced by CHPPR affects mitochondrial activity showing that these spheroid mitochondria display generation of proton motive force and oxidation ability. However, how this protein affects mitochondrial morphology at the molecular level is unknown so far and will be subject of further investigation.

MATERIALS AND METHODS

Sequence analysis and constructs generation

To obtain the coding sequence (cds) of the mouse ortholog of chicken CHPPR, BLAST analysis of mouse expressed sequence tags (EST) database was performed with the chick sequence at the National Center for Biotechnology Information (NCBI, Bethesda, MD) (Altschul et al., 1990); this screening identified an IMAGE cDNA clone 832381 as the putative mouse CHPPR ortholog. The complete nucleotide sequence of this clone was determined by automated sequencing using a 377 Perkin Elmer sequencer. All sequencing reactions were performed by using the BigDye terminator cycle sequencing kit (Perkin Elmer, Wellesley, MA). For sequence analyses, The "Sequencher" (Gene Codes Corp., Ann Arbor, MI) and the "GeneWorks®" (IntelliGenetics Inc., Campbell, CA) software packages were used. BLAST analysis demonstrated that this IMAGE clone encodes the mouse CHPPR and its sequence has been submitted to GenBank; its accession number is AF354708. The Mitoprot II protocol was used (Claros and Vincens, 1996) to assess probability of mitochondrial sorting.

The CHPPR myc-his tagged expression construct was generated by cloning the PCR generated cds fragment of chick CHPPR in frame with the 5′ end of the myc epitope cds of the pcDNA 3.1 myc-his vector (Invitrogen, San Diego, CA). A control Actin myc-his tagged construct was generated by cloning the PCR generated cds fragment of Actin sequence with GeneBank accession number NM_009606 in frame with the 5′ end of the myc epitope cds of the pcDNA 3.1 myc-his vector. The CHPPR flag-tagged expression construct was generated by cloning, in the pcDNA3.1 vector, the PCR generated cds fragment for the flag epitope (DYKDDDDK, single letter amino acid code) in frame with the 3′ end of chick CHPPR; a stop codon was inserted immediately after the codon specifying the C terminal K residue. The chick CHPPR–RFP (red fluorescent protein) chimera construct was generated by subcloning the chick CHPPR cds in frame with the 5′ end of the Ds2Red cds of the pDs2Red-N1 vector (Clontech, San Diego, CA). To obtain a doxycycline inducible chick CHPPR–RFP the cds encoding the protein chimera was subcloned in the pTRE2 vector. CHPPR–GFP (green fluorescent protein) chimeric construct were generated by subcloning, in the pcDNA3.1 vector, the entire CHPPR cds or its specific fragments in frame with a modified GFP cycle 3 mutant.

All constructs were sequenced in order to rule out any accidental mutation introduced by PCR amplification.

RNA isolation and Northern blot analysis

For Northern blot analysis, total RNA was extracted from cell cultures by using TRIzol reagent (Invitrogen) according to the manufacture's protocol. Total RNAs were electrophoresed through 1% agarose gels in the presence of formaldehyde and blotted onto Hybond N membranes (Amersham, Piscataway, NJ). Blot prehybridizations were performed at 65°C for 30 min in 333 mM NaH_2PO_4 pH 7.2, 6.66% sodium dodecyl sulphate, and 250 mg/ml denatured salmon sperm DNA. Blot hybridization was performed at 65°C for 18 h in the same solution containing 10^6 cpm/ml of denatured and labeled chick CHPPR cds probe spanning amino acid residues 1–62. After hybridization, the blots were washed twice at 65°C for 15 min in 0.2% sodium dodecyl sulphate, 2× SSPE and twice at 65°C for 15 min in 0.2% sodium dodecyl sulphate, 0.2× SSPE. Digital images of blots were acquired using the Cyclone phosphoimager (Packard instruments, Meridien, CT).

Cell culture and transfection

Chondrocyte cell culture methods are extensively described elsewhere (Altschul et al., 1990). Briefly, stage 29–30 chick embryo tibiae were removed, cleaned, washed in phosphate buffered saline (PBS), pH 7.2, and digested for 15 min at 37°C with 400 U/ml collagenase I and 0.25% trypsin. After sedimentation, the supernatant, containing tissue debris and perichondrium, was discarded and the pellet was digested for additional 45 min in the above dissociation buffer supplemented with 1,000 U/ml of collagenase II. Freshly dissociated chondrocytes were plated onto culture dishes. These cells were maintained in Coon's modified F12 medium with 10% FCS, supplemented with 5 mM glutamine, and cultured in adhesion for 3 weeks. During this time, chondrocytes dedifferentiate to fibroblast-like cells expressing type I collagen (Castagnola et al., 1988). Dedifferentiated cells were then transferred by 0.25% trypsin (Gybco BRL, San Diego, CA) digestion (in phosphate buffered saline) into 1% agarose coated petri dishes and cultured in suspension in a F12 medium with 10% FCS and with 5 mM Glutamine. COS7 and HeLa cells were cultured in Dulbecco's modified Eagle's medium supplemented with 10% FCS and with 5 mM Glutamine.

For transient transfection, cells were plated on poly-L-lysine-coated glass coverslips 16 h before transfection. Expression constructs were introduced into the cells using the Effectene transfection reagent (Qiagen, Hilden, Germany) according to the manufacturer's instructions.

To induce the expression of CHPPR–RFP chimera cloned into pTRE2, transfection was performed under serum-free conditions (Quarto et al., 1997) and 48 h later the medium was supplemented with Doxycycline.

Microscopic analysis of living cultured cells was performed at 37°C in a buffer containing NaCl 130 mM; KCl 5 mM; $MgSO_4$ 1.2 mM; KH_2PO_4 1.2 mM; $CaCl_2$ 1.2 mM; glucose 1.1 mg/ml; HEPES 25 mM pH 7.4.

Mitochondrial labeling

COS7 cells were labeled with 100 nM MitoTracker Orange CM-H2TMROS (Molecular Probes, Eugene, OR) following the manufacturer's instructions. Before labeling, hypertrophic chondrocytes were incubated in 1 mg/ml Hyaluronidase (Sigma, Saint Louis, MO) in phosphate buffered saline (PBS) for 10 min at 37°C. Subsequently, trypsin/EDTA (Sigma) was added and cells were incubated for another 10 min at 37°C. Enzymes were neutralized by addition of complete medium. The chondrocytes were centrifuged and resuspended in medium containing 100 nM MitoTracker Orange CM-H2TMROS (Molecular probes) according to manufacturer's instructions. Cells were fixed and permeabilized as described in the immunolocalization section.

Immunolocalization

Cells were fixed in 3% paraformaldehyde in PBS, pH 7.6 containing 2% sucrose for 5 min at room temperature. After rinsing in PBS, cells were permeabilized in a solution containing 20 mM HEPES pH 7.4, 300 mM sucrose, 50 mM NaCl, 3 mM $MgCl_2$, and 0.5% Triton X-100 for 5 min at 0°C. Nuclei were stained with Hoechst 33258 in PBS for 5 min at room temperature. Nonspecific binding was prevented by incubation with pure Goat serum for 30 min at 0°C. Slides were incubated with purified 10 mg/ml IgG1 of the anti c-myc (Evan et al., 1985) 9E10 monoclonal antibody (Development Hybridoma Bank), in PBS supplemented with 10% goat serum (antibody dilution buffer) for 2 h at 0°C. After extensive rinsing in PBS, slides were incubated for 30 min with FITC-conjugated goat anti-mouse antibody in antibody dilution buffer. Nuclei were stained with Hoechst 33258.

Fluorescence analysis

Routine observations were performed with a Zeiss Axiophot microscope equipped with a 100× Pan-Neofluar objective and with the following filter sets: 10, 15, and 02 to detect GFP/FITC (fluorescein iso-thiocyanate), RFP, and Hoechst 33258 respectively. Fluorescence images were recorded using a CCD camera (C5810 Hamamatsu). Image merging, composition, and printing were performed using Adobe Photoshop 5.0.

To acquire confocal images, samples were subjected to microscopy using a BioRad-MRC 1024 confocal microscope (60× objective, argon laser, sequential excitation at 468 and 580 nm). Digital images were acquired and processed using the BioRad Laser Pix software.

Immunoelectron microscopy

Pellets of COS7 cells, transfected with myc- or flag-tagged CHPPR, were fixed in 2% paraformaldehyde and 0.2% glutharaldehyde in PBS, embedded in 10% gelatin, infused with 2.3 M sucrose, and frozen in liquid nitrogen. Ultrathin cryo-sections were obtained with a Reichert-Jung Ultracut E with FC4E cryoattachment and collected on copper–formvar–carbon coated grids. Immunogold localization on ultrathin cryo-sections was performed as previously described (Slot and Geuze, 1984; Schiaffino et al., 1999). In particular, sections were immunostained with a rabbit anti-myc antibody (Santa Cruz, Santa Cruz, CA), or with a mouse anti-flag monoclonal antibody (Clone M2, Sigma) followed by 10-nm Protein A-gold. Sections were examined with Zeiss EM 10 and 902 electron microscopes.

Aequorin measurements

For aequorin measurements, HeLa cells (seeded onto 13 mm coverslips) were co-transfected with 3 μg pcDNA3 (control sample) and 1 μg mitochondrial matrix targeted Aequorin (mtAEQmut)/VR1012 or cytoplasmic targeted Aequorin (cytAEQ) (Montero et al., 2000). For the CHPPR sample, cells were transfected with 3 μg CHPPR–myc and 1 μg mtAEQmut/VR1012 or cytoplasmic targeted Aequorin (cytAEQ) using the calcium phosphate technique. Thirty-six hours after transfection, the coverslips with the cells were incubated with 5 μM coelenterazine for 2 h. All aequorin measurements were carried out in KRB (Krebs–Ringer modified buffer: 125 mM NaCl, 5 mM KCl, 1 mM $MgSO_4$, 1 mM Na_2HPO_4, 5.5 mM glucose, 20 mM $NaHCO_3$, 2 mM L-glutamine, 1 mM $CaCl_2$, and 20 mM HEPES, pH 7.4 at 37°C) in a 5% CO_2 atmosphere, and then transferred to the perfusion chamber.

One hundred micromolar histamine (Sigma-Aldrich, Saint Louis, MO) was added to the same medium. In order to obtain uncoupled mitochondria parallel control experiments were performed in the presence of 5 μM carbonyl cyanide m-chlorophenylhydrazone (CCCP). The aequorin experiments were terminated by lysing the cells with 100 mM digitonin (Sigma-Aldrich) in a hypotonic Ca^{2+}-rich solution (10 mM $CaCl_2$ in H_2O), thus discharging the remaining aequorin pool. The light signal was collected in a purpose-built luminometer and calibrated into $[Ca^{2+}]$ values as previously described (Chiesa et al., 2001).

Mitochondria membrane potential measurement

These measures were performed using 10 nM tetramethylrhodamine, methyl ester, perchlorate (TMRM) on a Zeiss confocal microscope (LSM 510). The signal was collected as total emission >570 nm. To distinguish control from the CHPPR–myc expressing cells these were cotransfected with a construct expressing GFP. Green emission was collected as emission from the range >505–535 nm.

RESULTS

Computer analysis prediction of CHPPR subcellular localization

To examine the subcellular localization of CHPPR we subjected the chick CHPPR amino acid sequence (Fig. 1A) to several subcellular protein localization prediction protocols available through the World Wide Web. Some of these protocols suggested possible mitochondrial localization for both the chick CHPPR and its human ortholog previously named KIAA0009. To confirm this, we also analyzed the mouse CHPPR ortholog. We explored the mouse EST database and found that the IMAGE clone 832381 was a putative mouse CHPPR ortholog. We determined its entire nucleotide sequence

A

```
MIRWFKCFMR MIFEQVGLNM ESVLWSSKPY GSSRSIVRKI GTNLSLIQCP  50
RVQFQLTSQA TEGNHPHQFR EDAVASFADV GWVAQEEGEV STRLRSEVWS 100
KTAQPLPGEL HQPGHSLGRQ DSVPNLLHEE PAPRSTVIAN EEAMQKISAL 150
ENELATLRAQ IAKIVILQEQ QNLTAAGLSP VASAAVPCVP PPPPPPPPPP 200
LPPPALQQSM SAIELIRERK NRKTNSGPIP TENGPKKPEI PNMLEILKDM 250
NSVKLRSVKK SSGDTKPKVA DPTDPAALIA EALKKKFAYR YRRDSQSESD 300
KVIPSLKRTR RPKWCCLDRT C                               321
```

B

```
ch-CHPPR    MIRWFKCFMRMIFEQVGLNMESVLWSSKPYGSSRSIVRKIGTNLSLIQCPRVQFQLTSQA   60
 m-CHPPR    MLGWIKCLMRMHFQRVGVSMQSVLWSGKPYGSSRSIVRKIGTNLSLIQCPRVQFQLTSHA   60
 h-CHPPR    MLGWIKRLIRMVFQQVGVSMQSVLWSRKPYGSSRSIVRKIGTNLSLIQCPRVQFQINSHA   60

ch-CHPPR    TEGNHPHQFREDAVASFADVGWVAQEEGEVSTRLRSEVWSKTAQPLPGELHQPGHSLGRQ   120
 m-CHPPR    TE-WSPAHSGEDAVASFADVGLVATEEGECSIRLRAEVSSKPPH--EDDPPCFEKPPSRH   117
 h-CHPPR    TE-WSPSHPGEDAVASFADVGWVAKEEGECSARLRTEVRSRPPL--QDDLLFFEKAPSRQ   117

ch-CHPPR    DSVPNLLHEEPAPRSTVIANEEAMQKISALENELATLRAQIAKIVILQEQQNLTAAGLSP   180
 m-CHPPR    TSFPSLSQDKPSPERT-LASEEALQKISALENELAALRAQIAKIVTLQEQQSPSAGCLD-   175
 h-CHPPR    ISLPDLSQEEPQLKTPLANEEALQKICALENELAALRAQIAKIVTQQEQQNLTAGDLD-   176

ch-CHPPR    VASAAVPCVPPPPPPPPPPLPPPALQQSMSAIELIRERKNRKTNSGPIPTENGPKKPEI   240
 m-CHPPR    -SSTSVT-VAPPPPPPPPPPLPLVLHQSTSALDLIKERREQRLSAGKTLATGHPKKPDM   233
 h-CHPPR    -STTFGTIPPHPPPPPPPLPPPALGLHQSTSAVDLIKERREKRANAGKTLVKNNPKKPEM   235

ch-CHPPR    PNMLEILKDMNSVKLRSVKKSSGDTKPKVADPTDPAALIAEALKKKFAYRYRRDSQSESD   300
 m-CHPPR    PNMLEILKDMNSVKLRSVKRSEKDVKPRPADTDHAAFI-AEALKKKFAYAHNSQGETERG   292
 h-CHPPR    PNMLEILKEMNSVKLRSVKRSEQDVKPKPVDATDPAALIAEALKKKFAYRYRSDSQDEVE   295

ch-CHPPR    KVIPSLKR--TRRPKW---CCLDRTC------------     321
 m-CHPPR    IPKPESEA--TSEPALFGPHILKSTGKMKALIENVPDS     328
 h-CHPPR    KGIPKSESEATSERVLFGPHMLKPTGKMKALIENVSDS     333
```

Fig. 1. Chick CHPPR (ch-CHPPR) amino acid sequence and comparison between CHPPR identified in chick, mouse, and human. ch-CHPPR amino acid sequence (**A**). Comparison between CHPPR identified in chick, mouse, and human: identical amino acid residues are boxed (**B**). The GeneBank accession numbers for the cDNA sequences coding CHPPR are as follow: chick, AF208489; mouse (m-CHPPR), AF354708; human (h-CHPPR), NM014637.

and confirmed the presence of the complete cds for mouse CHPPR. Comparison of the chick, mouse, and human CHPPR putative amino acid sequence revealed 50% amino acid conservation (Fig. 1B). In particular, the Mitoprot II algorithm (Claros and Vincens, 1996) revealed the presence of a putative mitochondrial import sequence with positively charged amino acid residues scattered at the N-terminal of CHPPR (not shown). This algorithm also predicted for chick, mouse, and human CHPPR a probability of mitochondrial sorting of 0.89, 0.99, and 0.98, respectively (Claros and Vincens, 1996). In all subsequent experiments, the chick CHPPR cDNA was used to generate expression constructs.

CHPPR is localized in mitochondria and promotes mitochondrial fission

To verify whether CHPPR is sorted to the mitochondria, a construct expressing myc tagged CHPPR (CHPPR–myc) was co-transfected together with a cytochrome oxidase subunit VIII-GFP (COX8-GFP) chimeric protein (Rizzuto et al., 1995) in dedifferentiated chick embryo chondrocytes. Immunofluorescence

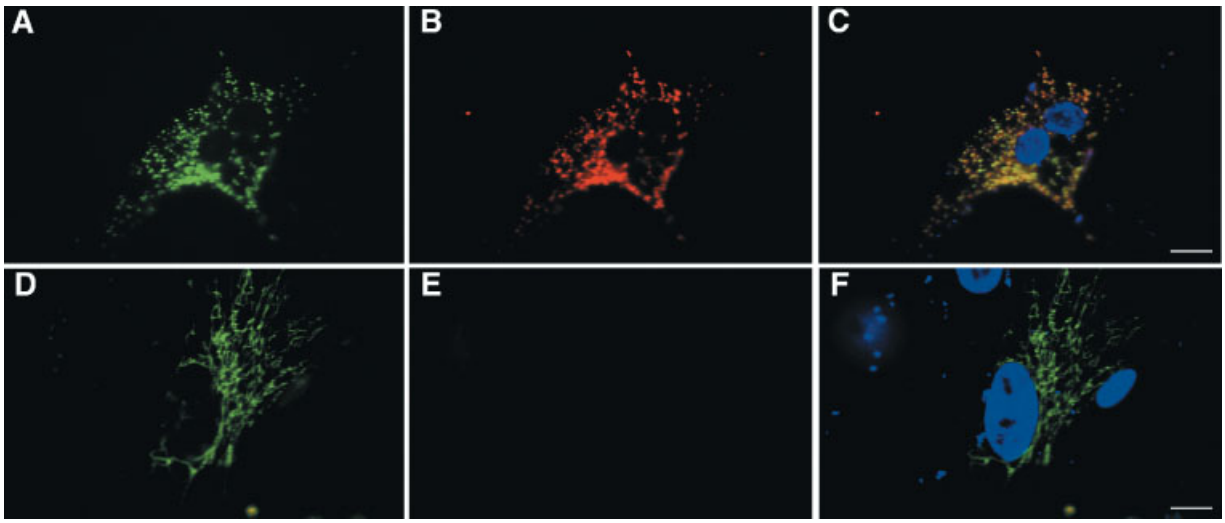

Fig. 2. Subcellular localization of CHPPR–myc and mitochondrial fragmentation in transfected dedifferentiated chondrocytes. Cells transfected with CHPPR–myc (**A**–**C**) or with empty expression vector (**D**–**F**) and with COX8-GFP (A–F) were fixed and treated with anti-myc antibody 24 h after transfection. CHPPR was detected with a TRICT-conjugated secondary antibody giving a red signal (B, C, E, F). COX8-GFP was visualized directly giving a green signal (A, C, D, F). The degree of spatial overlap in the distribution of the two proteins is shown by the respective merged images (C, F). Nuclei were stained with Hoechst 33258. Scale bar, 11.08 μm.

analysis of paraformaldehyde fixed cells, performed by using the anti myc antibody, revealed a punctate red signal corresponding to the tagged CHPPR (Fig. 2B). This signal colocalized with the green signal displayed by the COX8-GFP (Fig. 2A,C). As expected, control dedifferentiated chondrocytes cotransfected with the empty pcDNA 3.1 myc-his vector and with the COX8-GFP show only a typical green tubular mitochondrial network (Fig. 2D,F). As the CHPPR punctate or grain pattern is not characteristic for a mitochondrial protein, we were concerned about a possible, although unlikely, protein mistargeting, despite the fact that it did colocalize with a well-established mitochondrial marker such as the COX8-GFP. However, CHPPR–myc did not colocalize with proteins targeted to endoplasmic reticulum (ER), endosomes, lysosomes, peroxysomes, and Golgi cisternae (data not shown). To establish whether the colocalization of CHPPR–myc and COX8-GFP in a grain pattern was also present in cell types different from chick dedifferentiated chondrocytes, we cotransfected COS7 cells with the same constructs. Immunolocalization and fluorescence analysis displayed colocalization of the two signals in an identical grain pattern as observed in transfected chick dedifferentiated chondrocytes (Fig. 3). Colocalization of CHPPR–myc and COX8-GFP was further confirmed by confocal microscopy analysis (Fig. 4). To rule out a myc tag non-specific targeting to mitochondria a construct expressing an actin-myc chimera was generated and cotransfected in COS7 cells along with the COX8-GFP construct. Immunolocalization with the anti myc antibody and fluorescence analysis displayed no colocalization of the two signals excluding a myc epitope targeting to mitochondria (data not shown).

To precisely assess CHPPR–myc location in the mitochondria we investigated its subcellular distribution in transfected COS7 using immuno-gold techniques on ultrathin cryo-sections and electron microscopy analysis. The anti-myc antibody specifically labeled the mitochondria (Fig. 5A). When samples were examined at a higher magnification, we observed that 27% of gold particles were associated to mitochondrial surface while 73% labeled the intramitochondrial regions. A representative anti-myc labeled mitochondria at high magni-

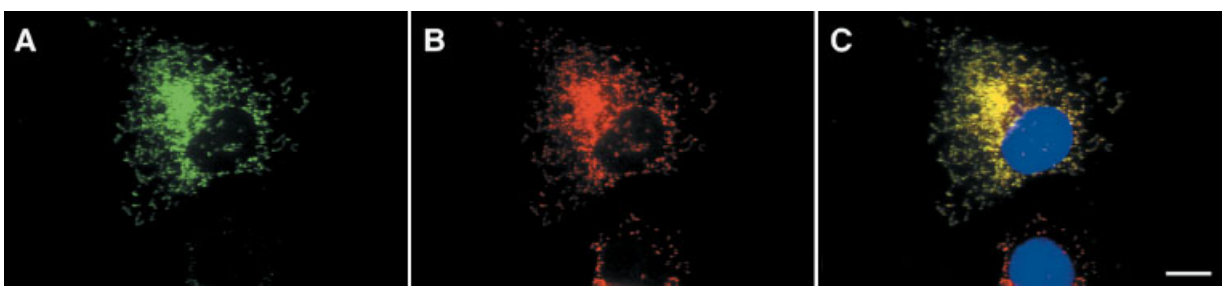

Fig. 3. Subcellular localization of CHPPR–myc and mitochondrial fragmentation in transfected COS7. Cells transfected with CHPPR–myc (**A**–**C**) and with COX8-GFP (A–C) were fixed and treated with anti-myc antibody 24 h after transfection. CHPPR was detected with a TRICT-conjugated secondary antibody giving a red signal (B, C). COX8-GFP was detected directly giving a green signal (A, C). The degree of spatial overlap in the distribution of the two proteins is shown by the merged image (C). Nuclei were stained with Hoechst 33258. Scale bar, 11.08 μm.

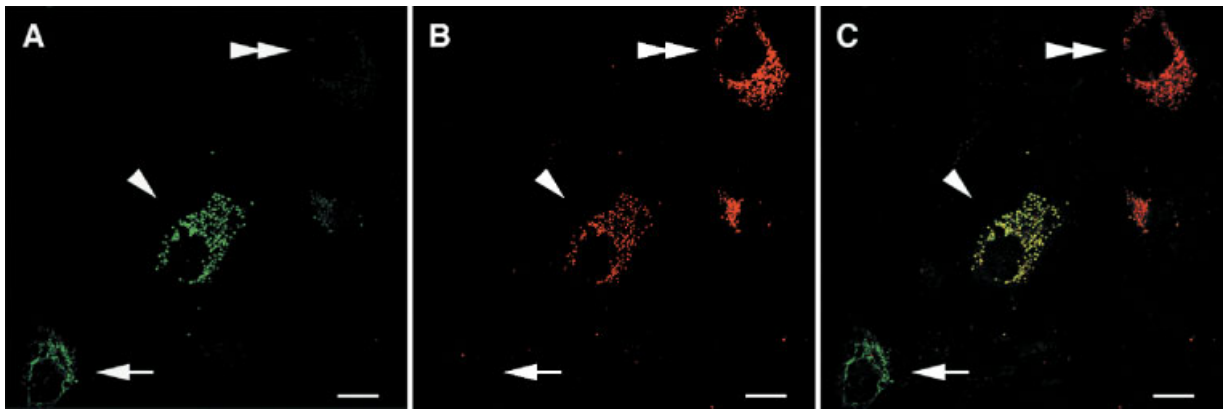

Fig. 4. Subcellular localization of CHPPR–myc and mitochondrial fragmentation in transfected COS7 as detected by confocal microscopy. Cells transfected with CHPPR–myc and with COX8-GFP were fixed and detected with anti-myc antibody 24 h after transfection. COX8-GFP was detected directly and gave a green signal (**A**, **C**) while CHPPR–myc was detected with a TRICT-conjugated secondary antibody giving a red signal (**B**, C). The degree of spatial overlap in the distribution of the two proteins is shown by the merged image (C). Arrow head indicates a cell expressing approximately equal amounts of CHPPR–myc and COX-8GFP; double arrow indicates a cell expressing higher amounts of CHPPR–myc than COX-8GFP; arrows indicate a cell expressing only COX8-GFP. The figure shows an optical confocal section acquired as described in Experimental Procedures. Scale bar, 12 μm.

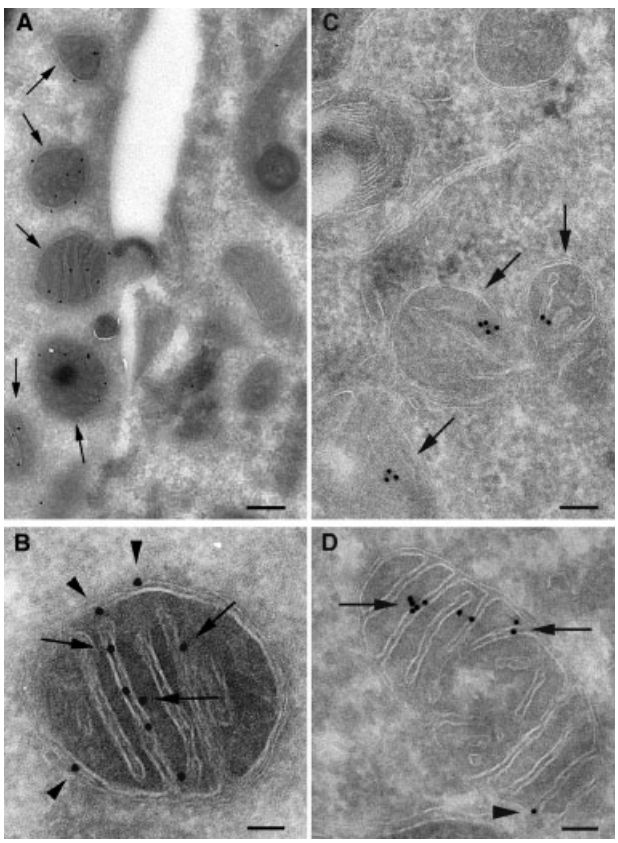

Fig. 5. Electron micrographs of ultrathin cryo-sections of CHPPR–myc and CHPPR-flag transfected COS7 cells. CHPPR–myc expressing cells are shown in (**A**) and (**B**); CHPPR-flag cells are shown in (**C**) and (**D**). Immunogold indicates mitochondria (arrows) in one of two adjacent cells (A) and (C). A high magnification image of a representative mitochondria in a CHPPR–myc expressing cell is shown in (B). A representative mitochondria in a CHPPR-flag expressing cell is shown in (D). Arrowheads indicate gold particles close to the mitochondrial outer surface and arrows indicate gold particles within mitochondria (B) and (D). Scale bars: 187 nm in (A); 83 nm in (B); 125 nm in (C) and (D).

fication is shown (Fig. 5B). Labeling specificity was confirmed by the absence of gold particles in cells transfected with empty vector (data not shown). To exclude a myc tag non-specific targeting to mitochondria we have also generated a further construct, expressing a CHPPR-flag chimera, and performed immuno electron microscopy using a specific anti flag monoclonal antibody. Analysis of cells transfected with this construct also showed a mitochondrial specific staining (Fig. 5C). In CHPPR-flag expressing cells, about 17% of gold particles were associated to mitochondrial surface and 83% to intramitochondrial structures; an anti-flag labeled mitochondria showing labeling both on the surface and of inner structures is shown (Fig. 5D).

To rule out the possibility of a change in mitochondrial morphology due to CHPPR over expression, we performed experiments in cells expressing low amounts of CHPPR. To control expression levels of CHPPR we applied a Tetracycline inducible expression system. Therefore, a CHPPR encoding DNA fragment, fused in frame with a red fluorescent protein (CHPPR–RFP), was subcloned in a pTRE2 vector. This construct was cotransfected with pTET ON and the construct encoding COX8-GFP in COS7 cells. As expected, spheroid mitochondria were detected at high levels of CHPPR–RFP expression, using 2 μg/ml doxycycline, (Fig. 6D,F). However, using these conditions we also detected a certain degree of accumulation of CHPPR–RFP in the cytoplasm (Fig. 6E,F). Interestingly, the transition from mitochondrial tubular network to mitochondrial spheroids or grains occurred even at low CHPPR–RFP levels using 0.2 μg/ml doxycycline (Fig. 6A,C).

Three-dimensional mitochondrial organization in living cells expressing CHPPR

To investigate whether the mitochondrial fission induced by CHPPR also occurs in living cells we subsequently examined COS7 cells microscopically, cotransfected with CHPPR–RFP (cloned in pDs2Red-N1 vector) and COX8-GFP and maintained in their culture environment. Under these conditions, cells

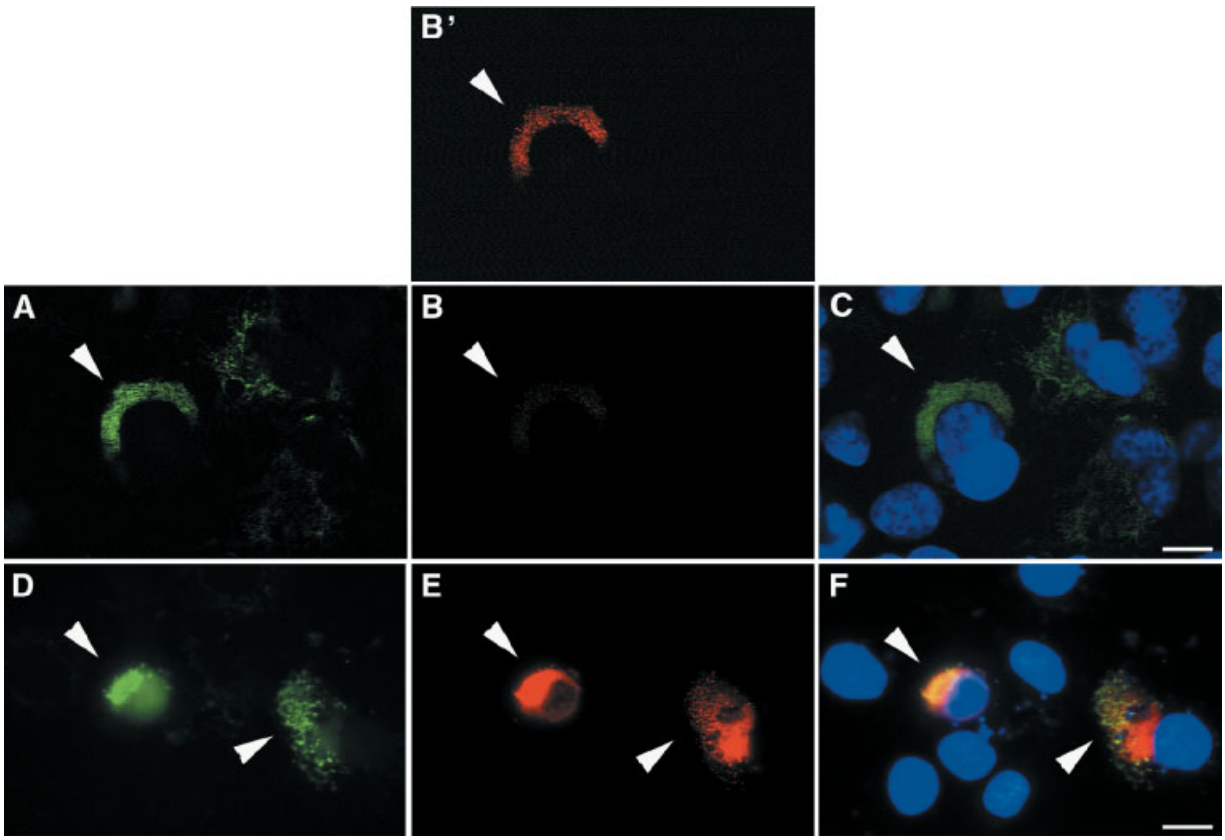

Fig. 6. Subcellular localization of CHPPR–RFP in transfected COS7 expressing CHPPR–RFP under the control of a doxycycline-responsive element. Cells were co-transfected with CHPPR–RFP (cloned in the pTRE2 vector), pTETON, and the COX8-GFP (**A**–**F**). To induce CHPPR–RFP expression medium was supplemented with 0.2 μg/ml (A–C) and 2 μg/ml (D–F) of Doxycycline 48 h after transfection. After another 12 h of incubation, cells were fixed and CHPPR–RFP and COX8-GFP were directly visualized as a red (B, **B′**, C, E, F) and a green signal (A, C, D, F), respectively. Images (B) and (E) were both acquired with 2 min exposure time. To better show the CHPPR–RFP signal in (B) luminance has been increased in (B′). The degree of spatial overlap in the distribution of the two proteins is shown by the respective merged images (C, F). Arrow heads point to cells displaying mitochondrial spheroids. Nuclei were stained with Hoechst 33258. Scale bar, 12 μm.

transfected with the empty pDs2Red-N1 vector displayed a diffuse pattern of RFP staining (Fig. 7C), whereas the mitochondrial tubular network was labeled by COX8-GFP only (Fig. 7C). Cells expressing CHPPR–RFP were characteristically stained in spheroid mitochondria (Fig. 7A). At a higher magnification, it is possible to identify subdomains within these grains (Fig. 7B).

Spheroid mitochondria in CHPPR expressing cells generate a proton motive force and are oxidation competent

In order to find out whether in cells expressing CHPPR mitochondria are able to retain close contacts with ER, to establish and maintain a proton motive force and whether they are able to carry on oxidative reactions we devised the following experiments.

To assess whether in cells expressing CHPPR mitochondria are able to retain close contact with ER, HeLa cells were cotransfected with a matrix targeted Aequorin along with the CHPPR–myc construct or with the empty vector and treated with histamine. This molecule induces the opening of IP_3-gated ER channels and the efflux of Ca^{2+} from the ER lumen to the cytoplasm. In correspondence of close ER–mitochondrial contacts a rapid uptake of Ca^{2+} by the mitochondria matrix, leading to an increase in mitochondrial matrix $[Ca^{2+}]$, take place only when proton gradient is established between the two sides of the inner mitochondrial membrane (Rizzuto et al., 1998). The timing and the extent of the mitochondrial matrix $[Ca^{2+}]$ response to histamine, detected in CHPPR–myc transfected cells, was comparable with that of control cells, demonstrating that over expression of this protein does not cause disruption of mitochondrial–ER close contacts or mitochondrial damages and impairment of the proton motive force (Fig. 8A). As expected, when the same experiment was performed in the presence of the uncoupling agent CCCP, the spike of mitochondrial matrix $[Ca^{2+}]$ was abolished (data not shown). In order to verify that changes in cytosolic $[Ca^{2+}]$ occur after histamine stimulation we used as a read out system a cytosolic Aequorin (cytAEQ). No differences were observed, between CHPPR–myc and vector transfected cells, in the timing and extent of the cytoplasmic $[Ca^{2+}]$ response to histamine treatment (Fig. 8B).

To directly address whether mitochondrial membrane potential in CHPPR expressing cells is comparable with

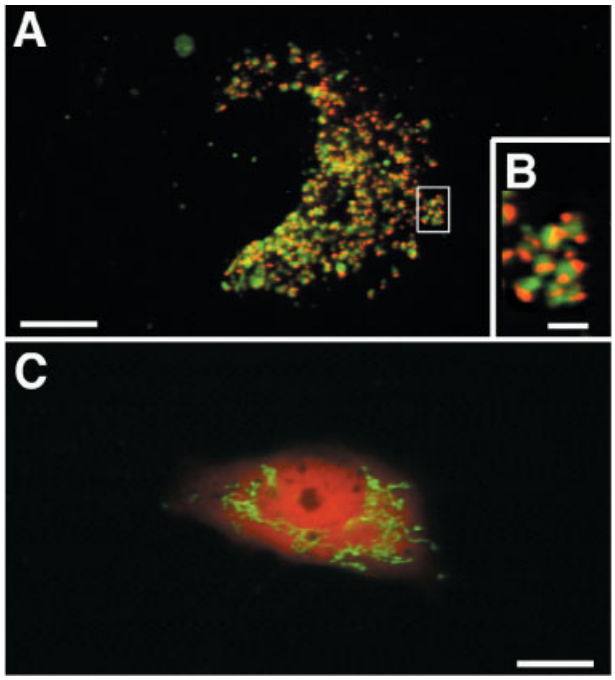

Fig. 7. Mitochondrial fragmentation in living COS7 expressing CHPPR–RFP. Cells transfected with CHPPR–RFP (**A**, **B**) or with empty expression vector (mock, **C**) and with COX8-GFP (A–C) were analyzed 24 h after transfection as indicated in Experimental Procedures. CHPPR–RFP (A, B) and the RFP, expressed by the empty vector (C), were visualized directly as a red signal while COX8-GFP was visualized directly as a green signal (A–C). A higher magnification of the rectangular area indicated in A is shown in B. Scale bars: 13.5 μm in (A and C), 1.8 μm in (B).

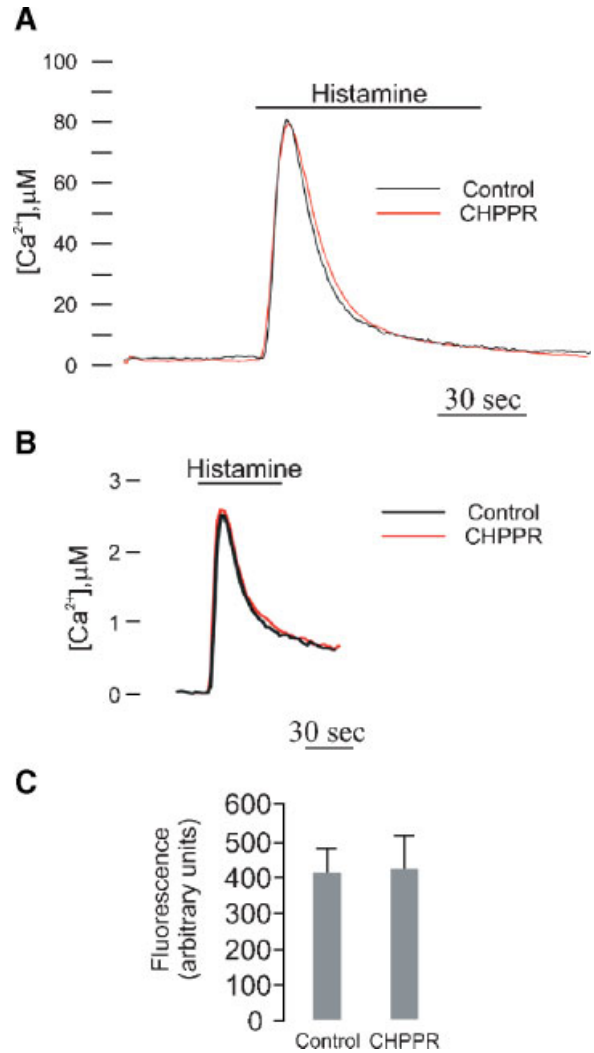

Fig. 8. Mitochondria of CHPPR expressing cells are able to import Ca^{2+} from mitochondria–ER close contacts and to maintain a proton gradient. Effect of histamine on $[Ca^{2+}]$ changes in the mitochondrial matrix (**A**) or in the cytoplasm (**B**) of HeLa cells is shown. These were transfected with CHPPR–myc (red line) or with empty expression vector (black line) and with a mtAEQmut in (A) or with CytAEQ in (B). Forty-eight hours after transfection cells were stimulated with histamine 100 μM. $[Ca^{2+}]$ was detected as described in Materials and Methods. Mitochondrial membrane potential was measured using TMRM by confocal microscopy as described in Materials and Methods (C).

control cells, this was measured by confocal microscopy using TMRM whose accumulation in mitochondria is driven by membrane potential. To distinguish control cells from CHPPR expressing cells a GFP construct was cotransfected with CHPPR–myc. Figure 8C shows that TMRM fluorescence intensity obtained from CHPPR expressing cells is similar to that obtained from control cells.

To assess whether mitochondria of CHPPR expressing cells are able to carry on oxidative reactions we took advantage of the MitoTracker Orange (CM-H2TMROS). This mitochondrial selective probe is converted upon oxidation in the fluorescent CMTMROS form, allowing labeling of actively respiring mitochondria. COS7 cells were incubated 24 h after transfection, with CHPPR–myc or with the empty vector, in medium supplemented with MitoTracker Orange (CM-H2TMROS). Fluorescence analysis showed a grain pattern of colocalized MitoTracker Orange (in its oxidized CMTMROS form) and myc signal in cells transfected with the CHPPR–myc (Fig. 9A) whereas mitochondria, labeled with a MitoTracker Orange, presented a thread like structure in cells transfected with the empty vector (Fig. 9B).

Identification of the CHPPR domains responsible for mitochondrial import and for the mitochondrial network–spheroid transition

In order to identify within the primary structure of the protein those regions responsible for mitochondrial import and mitochondrial fission a series of chimeric constructs were generated incorporating only specific portions of the CHPPR cds fused to GFP (Fig. 10). Residues 1–62, including the putative CHPPR mitochondrial import sequence, were fused in frame to the N-terminal of GFP to verify its effectiveness and specificity in protein sorting (construct A, Fig. 10). Cells transfected with this construct display colocalization of the chimera with MitoTracker Orange in the mitochondrial tubular network demonstrating that the CHPPR mitochondrial import sequence is located at the N-terminal of the protein and that this is unable to induce thread-grain mitochondrial transition (Fig. 10A). This chimeric polypeptide was used to target to mitochondria several

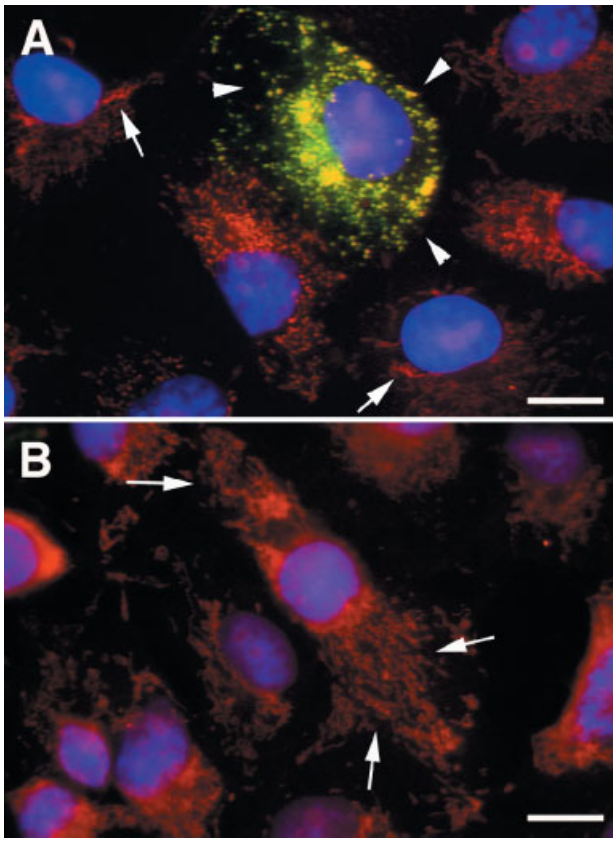

Fig. 9. Mitotracker Orange oxidation by fragmented mitochondria in COS7 expressing CHPPR–myc. Cells transfected with CHPPR–myc (**A**) or with empty expression vector (mock, **B**). Fourty eight hours after transfection, cells were labeled with MitoTracker Orange for 45 min as described in Experimental Procedures. After labeling, cells were washed, fixed, and treated with anti-myc antibody. CHPPR was visualized as a green signal with a FITC-conjugated secondary antibody while Mitotracker Orange was directly visualized as a red signal. Arrow heads point to mitochondrial spheroids; arrows indicate some tubular mitochondria. The degree of spatial overlap in the distribution of the two signals is shown by the respective merged images. Nuclei were stained with Hoechst 33258. Scale bar, 13.3 μm.

portions of the CHPPR protein in order to explore their ability to induce fission (Fig. 10).

As a first step to locate the region responsible for mitochondrial fragmentation, two constructs were generated: construct B, bearing the amino terminal 1–188 residues fused to the N-terminal of a GFP (Fig. 10) and construct C, coding for the 1–62 CHPPR–GFP fused to the N terminal of the CHPPR region spanning amino acid residues 182–321 (Fig. 10). Expression of construct B showed that although the chimera localized in mitochondria it was unable to induce fission (Fig. 10B) whereas construct C was both localized in mitochondria and able to induce a thread–grain transition (Fig. 10C). To verify whether this region, spanning amino acid residues 182–321, required mitochondrial sorting to be effective in fission, we generated the construct D: identical to construct C but lacking the mitochondrial importing sequence (Fig. 10). This chimera was both unable to localize in mitochondria, as expected, and unable to disrupt the mitochondrial tubular network (Fig. 10D). Within the region spanning amino acid residues 182–321 we identified two subregions to be further assayed for their fission ability: the first one containing the region spanning amino acid residues 182–212, including the poly-proline region, and the second one spanning residues 206–321, C-terminal to the poly-proline region (Fig. 10). Two distinct constructs were made fusing these two regions to the C-terminal of 1–62 CHPPR–GFP: constructs E and F (Fig. 10). Although both chimerae were sorted to mitochondria, as shown by colocalization with Mito Tracker Orange, none of them was able to promote mitochondrial fission (Fig. 10E,F). A further construct generated fusing the region spanning amino acid residues 251–321 to the C-terminal of 1–62 CHPPR–GFP was also unable to induce a thread-grain transition (not shown). From these experiments, we concluded first, that both the poly-proline and the region located to its C-terminal side, are necessary to promote fission but not sufficient, if expressed separately, and second, that the fission domain begins with the poly-proline region at N-terminal and extends for some residues toward the C-terminal of CHPPR. In order to restrict the C-terminal boundary of this domain, two further constructs were made, fusing to the C-terminal of 1–62 CHPPR–GFP, the regions spanning from residue 182 to residues 257 (not shown) and 309, construct G (Fig. 10). Among these two constructs, only construct G was able to induce mitochondrial fission (Fig. 10G). This result was also confirmed by confocal microscopy (Fig. 11A–C). Taken together these experiments demonstrated that the CHPPR domain necessary and sufficient to promote a mitochondrial thread-grain transition is within residues 182–309.

To verify whether high chimeric transcript levels correlated with fission ability of specific constructs, a Northern blot was performed with RNA extracted from transfected COS7 cells. This analysis demonstrated that endogenous CHPPR mRNA is undetectable in cells transfected with the empty vector (Fig. 12). Northern analysis also showed that the fission competent construct C (Fig. 10) expresses comparable, or even lower level of chimeric mRNA, when compared to three constructs incompetent for fission (Fig. 12). These fission

Fig. 10. Identification of the CHPPR domains responsible for mitochondrial import and fission. COS7 cells were transfected with constructs shown in the lower right part: (**A**) construct A; (**B**) construct B; (**C**) construct C; (**D**) construct D; (**E**) construct E; (**F**) construct F; (**G**) construct G. After 48 h from transfection, cells were labeled with MitoTracker Orange for 45 min as described in Experimental Procedures. After labeling, cells were fixed and subjected to conventional epifluorescence microscopy (A–G). Chimeric CHPPR–GFP proteins were directly visualized as a green signal while Mitotracker Orange was directly visualized as a red signal. The degree of spatial overlap in the distribution of the two signals is shown by the merged images (A–G). Arrows point to cells displaying mitochondrial fragmentation. Nuclei were stained with Hoechst 33258. Scale bar, 13.3 μm. In the lower right part, the position of relevant amino acid residues is indicated and different regions of CHPPR are represented by a different filling pattern. The poly-proline region is shown as a black filled box. GFP is represented by a white rounded rectangle. N-terminal protein ends are to the left side. Arrows indicate fission competent constructs.

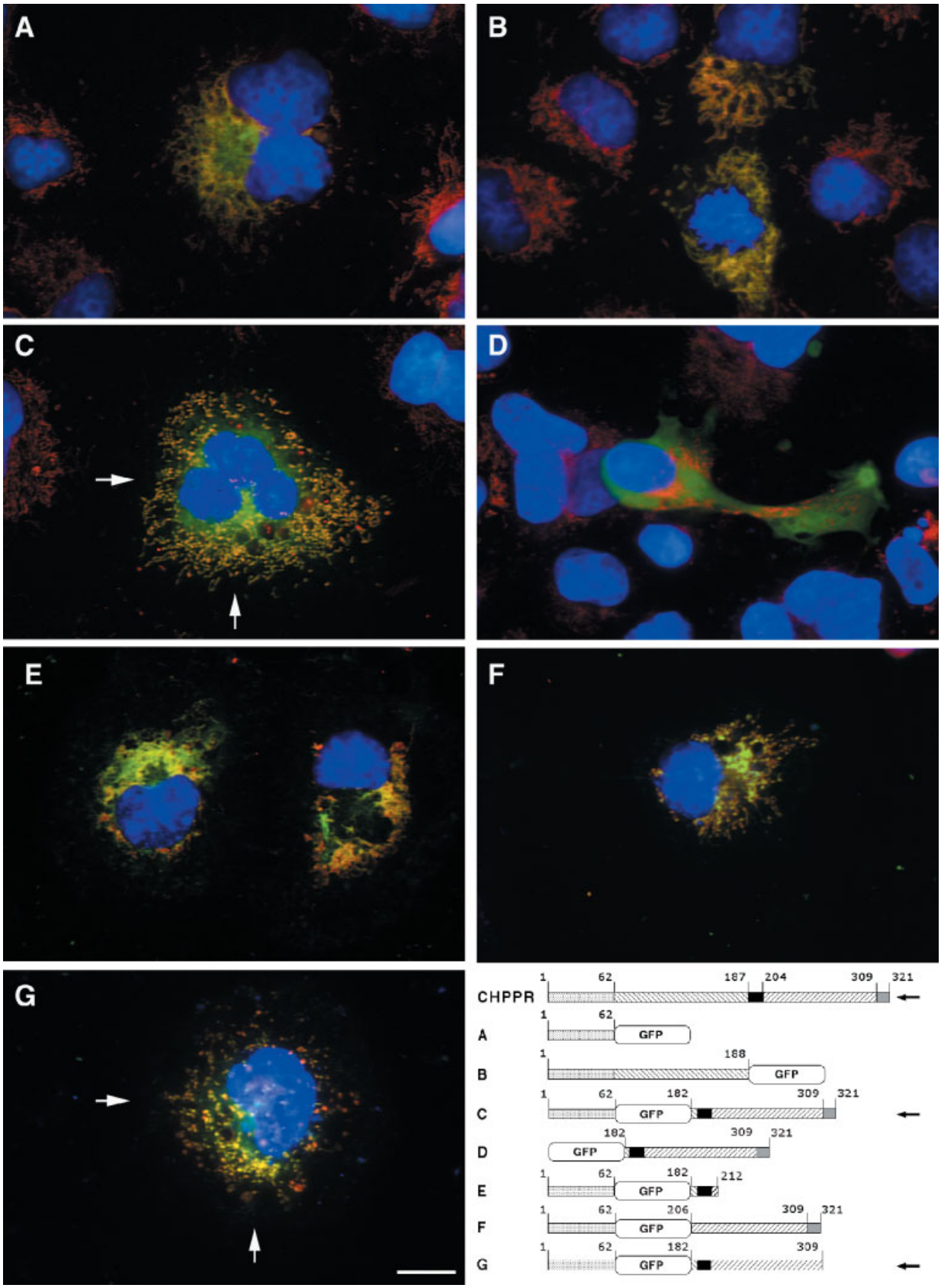

Fig. 10.

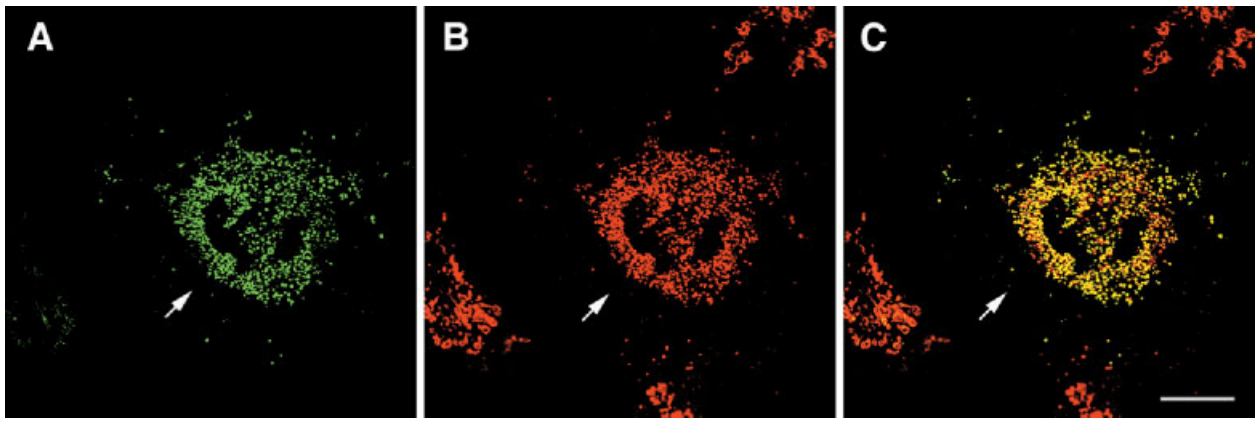

Fig. 11. Mitochondrial fragmentation induced by the CHPPR fission domain as detected by confocal microscopy. COS7 cells were transfected with construct G shown in Figure 10. After 48 h from transfection, cells were labeled with MitoTracker Orange for 45 min as described in Experimental Procedures. After labeling cells were fixed and subjected to confocal imaging (**A**–**C**). The chimeric CHPPR–GFP protein bearing the fission domain was directly visualized as a green signal (A) while Mitotracker Orange was directly visualized as a red signal (B). The degree of spatial overlap in the distribution of the two signals is shown by the merged image (C). The figure shows an optical confocal section acquired as described in Experimental Procedures. Arrows point to a cell displaying mitochondrial fragmentation. Scale bar, 12 μm.

incompetent constructs were: CHPPR 251–321 amino acid residues fused to the C-terminal of 162 CHPPR–GFP (not shown) and constructs A and F (Fig. 10).

Three-dimensional mitochondrial organization in hypertrophic chondrocytes

Since embryonic chick cartilage and hypertrophic chondrocytes express CHPPR (Tonachini et al., 2002), we expected to find spheroid mitochondria in these cells. Therefore we investigated the three-dimensional mitochondrial structure in hypertrophic chondrocytes by using MitoTracker Orange (CM-H2TMROS). Confocal imaging of these samples, showed that the fluorescent signal generated by the oxidized form of MitoTracker (CMTMROS) was distributed in a grain pattern within these cells, indicating spheroid morphology of mitochondria (Fig. 13).

DISCUSSION

We have recently identified a chick cDNA encoding a 321 amino acid protein referred to as chondrocyte protein with a poly-proline region (CHPPR), which is expressed in hypertrophic chondrocytes, in developing hypertrophic cartilage and to a lower extent in other chick embryonic tissues (Tonachini et al., 2002). In this study, we report that chick, mouse, and human CHPPR overall share 50% sequence identity. A region of CHPPR, spanning amino acid residues 1–62, fused to the N-terminal of GFP is able to localize the chimeric protein in mitochondria demonstrating that this region contains a mitochondrial import sequence. Furthermore, experiments of co-expression of CHPPR fused to a myc epitope (CHPPR–myc) and the mitochondrial marker COX8-GFP (Rizzuto et al., 1995) demonstrate that the entire CHPPR is sorted to mitochondria not only in dedifferentiated chick embryo chondrocytes but also in other cell types such as COS7, HeLa, and 293T cells. Since COS7 cells are much easier to obtain and to transfect, this cell line was used during most subsequent experiments.

Immunoelectron microscopy shows that CHPPR is present in close proximity to the mitochondrial inner and, at a much lesser extent, close to the outer membranes regardless of the epitope used to tag the protein. In addition, these experiments show that labeled mitochondria do not display ultra-structural alterations. However, it should be noticed that labeling on the mitochondrial surface might reveal proteins caught during the translocation process.

The most striking observation in CHPPR transfected cells is the presence of spheroid mitochondria instead of the tubular mitochondrial network as detected in control non-transfected cells. Furthermore as this mitochondrial fission also occurs in chicken cells, transfected with chick CHPPR, a toxic effect due to the expression of a species-unrelated protein is excluded. Since CHPPR mitochondrial localization and this change in the three-dimensional mitochondrial organization are also observed in living cells, we rule out the possibility that these phenomena are due to a fixation artifact.

To verify whether CHPPR expression and the organelle spheroidal shape are compatible with normal mitochondrial activities we have investigated the ability of transfected cells to generate a proton gradient and to oxidize an appropriate substrate. Since it has been shown that after histamine stimulation and in the presence of a proton gradient, ER released Ca^{2+} is transported in the mitochondrial matrix (Rizzuto et al., 1998) we measured [Ca^{2+}] modulation in this compartment of CHPPR transfected cells. This experiment shows that the cell behavior was not significantly different from control cells transfected with an empty vector. Therefore, CHPPR expression does not affect proton gradient and Ca^{2+} transport in the mitochondrial matrix and close ER–mitochondrial contacts are retained when spheroid mitochondria are present in the cell instead of the thread network. These contacts were shown to be determinants of mitochondrial Ca^{2+} responses (Lawrie et al., 1996). An independent and direct evidence confirming the existence of a proton

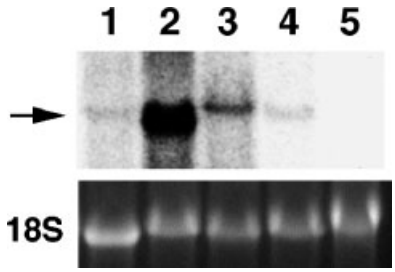

Fig. 12. Detection of chimeric CHPPR–GFP mRNAs in transfected COS7 cells by Northern blot analysis. RNA extracted from COS7 cells transfected with constructs shown in Figure 10: **C** (lane 1); **A** (lane 2); **F** (lane 3); with a construct coding for CHPPR acid residues 251–321 fused to the C-terminal of construct 1–62 CHPPR–GFP (lane 4) and with the empty vector pcDNA 3.1 (lane 5). RNA was extracted 48 h from transfection and about 10 μg of total RNA were loaded in each lane. A DNA fragment of CHPPR cds spanning amino acid residues 1–62 was used as probe. The arrow points to CHPPR transcripts. The Bottom part shows the 18S rRNA region of the gel before blotting as control for RNA loading.

gradient in mitochondria of CHPPR expressing cells, was obtained by measures of mitochondrial membrane potential using TMRM. Furthermore, we show that spheroid mitochondria of CHPPR expressing cells can be labeled with mitotracker orange. This cell-permeant dye in its CM-H2TMROS form is not fluorescent. In contrast, in metabolically active cells it is sequestered in mitochondria and becomes fluorescent following oxidization to CMTMROS. Therefore by using three distinct assays we show that spheroid mitochondria in CHPPR expressing cells are functionally competent.

Since CMV-induced over expression of CHPPR mRNA might result in an abnormal amount of protein responsible for the disruption of the mitochondrial network via a non-specific mechanism, we have used an inducible expression system allowing regulation of the amount of CHPPR synthesized by the transfected cells. We show that mitochondrial fission also occurs with low or barely detectable amount of CHPPR–RFP. Here we demonstrate that a specific domain in the C-terminal half of CHPPR, spanning amino acid residues 182–309 and containing the poly-proline region, is responsible for mitochondrial fission. In fact the expression of a mitochondrial-targeted GFP chimera fused to this domain, promotes a mitochondrial thread-grain transition whereas GFP-CHPPR chimeric proteins lacking this domain, or bearing only a portion of it (either the poly-proline region or the polypeptide portion immediately C-terminal to this region), are unable to induce this process. Furthermore we show that a construct containing the specific fission domain is not expressed at higher levels than constructs lacking this domain, ruling out again a toxic effect due to over expression of the corresponding protein.

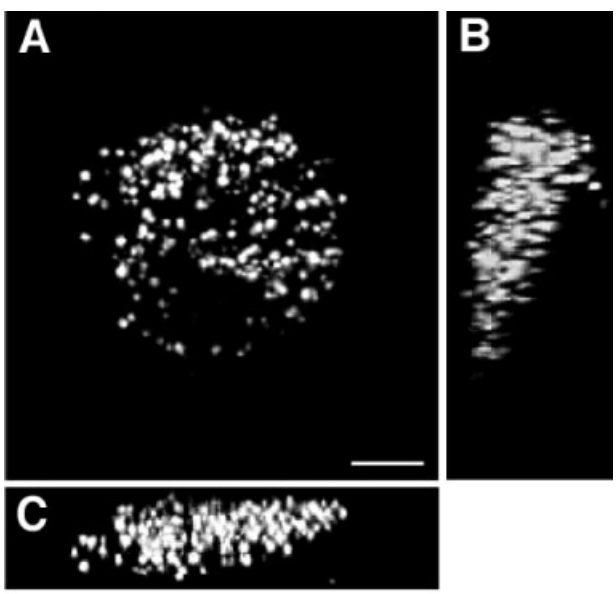

Fig. 13. Mitochondrial morphology of chick hypertrophic chondrocytes. Cultured hypertrophic chondrocytes were labeled 45 min with Mitotracker Orange. After labeling, cells were fixed and subjected to confocal imaging. Optical sections with an increment along Z-axis of 0.15 μm steps were acquired. The projected images on the x–y; y–z, and x–z planes are shown respectively in (**A**), (**B**), and (**C**). Scale bar, 6 μm.

These observations demonstrate that CHPPR induces mitochondrial fission via a specific mechanism leading to the hypothesis that cells expressing endogenous CHPPR should show spheroid mitochondria rather than a tubular mitochondrial network. To test this hypothesis we have investigated the mitochondrial structure in hypertrophic chondrocytes by using a mitochondrial-specific probe. This labeling experiment confirmed that spheroid mitochondria are indeed present in hypertrophic chondrocytes.

As far as we know this is the first report showing that cultured hypertrophic chondrocytes differ from other cell types in their three-dimensional mitochondrial organization. Furthermore, we demonstrate that, at least in vitro, a thread–grain transition occurs during maturation from dedifferentiated chondrocytes to hypertrophic chondrocytes. In fact dedifferentiated chondrocytes, expressing only negligible amounts of CHPPR mRNA (Tonachini et al., 2002), display a mitochondrial thread network, whereas hypertrophic chondrocytes, expressing high levels of endogenous CHPPR mRNA and protein (Tonachini et al., 2002), display spheroid mitochondria.

Mitochondrial morphology is dynamic and depends on two opposing processes: fission and fusion (Nunnari et al., 1997; Rizzuto et al., 1998). However these two mitochondrial processes have not yet been completely solved at the molecular levels (Griparic and van der Bliek, 2001; Westermann, 2002). Since CHPPR shares no homology with any protein present in the NCBI and EMBL database, or with known proteins regulating mitochondrial fission or fusion, it might be an additional and novel component of the multi molecular mechanism responsible for regulating mitochondrial morphology. On the other hand, cells transfected with CABC1, a human mitochondrial protein similar to the yeast chaperone of the bc1 complex, display spheroid mitochondria (Iiizumi et al., 2002). Therefore, we cannot rule out that CHPPR might specifically interact with some respiratory complex and that this interaction is in turn responsible of the mitochondrial fragmentation. The localization of CHPPR close to mitochondrial membranes, as detected by immunoelectron microscopy, is compatible with both hypotheses.

Lack of homology of CHPPR with Yeast and *Drosophila* proteins suggests that CHPPR rather than having a key function in the mitochondrial fission machinery might play a facilitative/regulative role or that its function is carried out by other non-vertebrate proteins that might share only a structural homology. It should be pointed out that the only module/motif that we have been able to identify in CHPPR, using available informatics tools, is the poly-proline region included in the fission domain and necessary for its function. Poly-proline regions have been demonstrated to be responsible for establishing protein–protein interaction (Williamson, 1994; Kay et al., 2000). Therefore, if a functional non-vertebrate CHPPR homologue exists, it is likely to share this module.

In conclusion, our study shows that CHPPR is a mitochondrial protein containing a specific domain able to induce, albeit by an unknown mechanism, mitochondrial fission without loss of functional activity of these organelles.

ACKNOWLEDGMENTS

We thank Laura Amabile for technical assistance, Marina Fabbi, and Annemiek Beverdam for critical reading of the manuscript and constructive discussions.

LITERATURE CITED

Altschul SF, Gish W, et al. 1990. Basic local alignment search tool. J Mol Biol 215:403–410.

Castagnola P, Dozin B, et al. 1988. Changes in the expression of collagen genes show two stages in chondrocyte differentiation in vitro. J Cell Biol 106:461–467.

Chiesa A, Rapizzi E, et al. 2001. Recombinant aequorin and green fluorescent protein as valuable tools in the study of cell signaling. Biochem J 355:1–12.

Claros MG, Vincens P. 1996. Computational method to predict mitochondrially imported proteins and their targeting sequences. Eur J Biochem 241:779–786.

Evan GI, Lewis GK, et al. 1985. Isolation of monoclonal antibodies specific for human c-myc proto-oncogene product. Mol Cell Biol 5: 3610–3616.

Griparic L, van der Bliek AM. 2001. The many shapes of mitochondrial membranes. Traffic 2:235–244.

Iiizumi M, Hirofumi A, et al. 2002. Isolation of a novel gene, *CABC1*, encoding a mitochondrial protein that is highly homologous to yeast activity of bc1 complex. Cancer Res 62:1246–1250.

Kay BK, Williamson MP, et al. 2000. The importance of being proline: The interaction of proline-rich motifs in signaling proteins with their cognate domains. Faseb J 14:231–241.

Lawrie AM, Rizzuto R, et al. 1996. A role for calcium influx in the regulation of mitochondrial calcium in endothelial cells. J Biol Chem 271:10753–10759.

Montero M, Alonso MT, et al. 2000. Chromaffin-cell stimulation triggers fast millimolar mitochondrial C^{2+} transients that modulate secretion. Nat Cell Biol 2:57–61.

Nomura N, Miyajima N, et al. 1994. Prediction of the coding sequences of unidentified human genes. I. The coding sequences of 40 new genes (KIAA0001–KIAA0040) deduced by analysis of randomly sampled cDNA clones from human immature myeloid cell line KG-1. DNA Res 1:27–35.

Nunnari J, Marshall WF, et al. 1997. Mitochondrial transmission during mating in *Saccaromyces cerevisiae* is determined by mitochondrial fusion and fission and the intramitochondrial segregation of mitochondrial DNA. Mol Biol Cell 8:1233–1242.

Quarto R, Campanile G, et al. 1997. Modulation of commitment, proliferation, and differentiation of chondrogenic cells in defined culture medium. Endocrinology 138:4966–4976.

Rizzuto R, Brini M, et al. 1995. Chimeric green fluorescent protein as a tool for visualizing subcellular organelles in living cells. Curr Biol 5:635–642.

Rizzuto R, Pinton P, et al. 1998. Close contacts with the endoplasmic reticulum as determinants of mitochondrial Ca^{2+} responses. Science 280:1763–1766.

Schiaffino MV, d'Addio M, et al. 1999. Ocular albinism: Evidence for a defect in an intracellular signal transduction system. Nat Genet 23:108–112.

Slot JW, Geuze HJ. 1984. Gold markers for single and double immunolabeling of ultrathin cryosections. In: Polak JM, Varndell IM, editors. Immunolabeling for electron microscopy. Amsterdam, NL: Elsevier. pp 129–142.

Tonachini L, Monticone M, et al. 2002. Chondrocyte protein with a poly-proline region (CHPPR) is a novel protein expressed by chondrocytes in vitro and in vivo. Biochim Biophys Acta 1577: 421–429.

Westermann B. 2002. Merging mitochondria matters: Cellular role and molecular machinery of mitochondral fusion. EMBO Rep 3: 527–531.

Williamson MP. 1994. The structure and function of proline-rich regions in proteins. Biochem J 297:249–260.